Arch. Mech., **69**, 3, pp. 223–241, Warszawa 2017

# Modeling Gum Metal and other newly developed titanium alloys within a new class of constitutive relations for elastic bodies

V. KULVAIT[1)], J. MÁLEK[1)], K. R. RAJAGOPAL[2)]

[1)] *Mathematical Institute*
*Faculty of Mathematics and Physics*
*Charles University*
*Sokolovská 83, 186 75 Prague, Czech Republic*
*e-mail: malek@karlin.mff.cuni.cz*

[2)] *Department of Mechanical Engineering*
*Texas A&M University*
*College Station, TX, 77843, U.S.A.*

Many titanium alloys and even materials such as concrete exhibit a nonlinear relationship between strain and stress, when the strain is small enough that the square of the norm of the displacement gradient can be ignored in comparison to the norm of the displacement gradient. Such response cannot be described within the classical theory of Cauchy elasticity wherein a linearization of the nonlinear strain leads to the classical linearized elastic response. A new framework for elasticity has been put into place in which one can justify rigorously a nonlinear relationship between the linearized strain and stress. Here, we consider one such model based on a power-law relationship. Previous attempts at describing such response have been either limited to the response of one particular material, e.g. Gum Metal, or involved a model with more material moduli, than the model considered in this work. For the uniaxial response of several metallic alloys, the model that is being considered fits experimental data exceedingly well.

**Key words:** titanium alloys, modeling, implicit constitutive theory.



## 1. Introduction

In material science there is an ongoing effort to develop new titanium alloys in virtue of their beneficial properties. An illustrative example is Gum Metal[1], a material that has been developed by Toyota Central R&D Labs. Gum Metal is a designation for a class of beta titanium alloys with unique elastic properties that include low Young's modulus, high strength and high yield strain

[1]GUMMETAL is a trademark owned by the Toyota Tsusho Material Inc. company (as of 2017).

in comparison to other conventionally used materials and titanium alloys, see [1]. Cold swagged Gum Metal has a reversible nonlinear elastic response up to the strains of 2.5%, which is referred to as super elasticity, see [2, 3].

Gum Metal, however, is not the only titanium alloy that exhibits a nonlinear relationship between the strain and the stress, when the strain is small enough that the square of the norm of the displacement gradient can be neglected in comparison to the norm of the displacement gradient. Such nonlinear elastic behavior seems to be typical for many beta-phase titanium alloys, see [4–6]. Their nonlinear response cannot be described within the context of any Cauchy elastic model (and hence any Green elastic model) as the linearization of a nonlinear constitutive expression for the stress leads to the classical linearized elastic model which is a linear relationship between the stress and linearized strain. While the response can be curve-fitted by using a nonlinear relationship between the stress and the strain, one cannot justify it or show that it follows from the linearization of a model to describe elastic response. Recently, Rajagopal [7] (see also [8]) recognized that the class of bodies that are elastic, if by elastic body one understands the body that is incapable of dissipation and which converts mechanical working into thermal energy (heat), is far larger than Cauchy elastic bodies. He proposed a class of implicit relationships between the Cauchy stress and deformation gradient to describe elastic response, Cauchy elasticity being a very small special sub-class of them. Rajagopal and Srinivasa [9, 10] provided a rigorous thermodynamic basis for the same. In the case of isotropic elastic bodies described by implicit constitutive relations, we have the relationship

$$\boldsymbol{G}(\rho, \boldsymbol{T}, \boldsymbol{B}) = \boldsymbol{0}, \tag{1.1}$$

where $\rho$ denotes the density, $\boldsymbol{T}$ is the Cauchy stress tensor and $\boldsymbol{B}$ is the left Cauchy-Green strain tensor, i.e., $\boldsymbol{B} = \boldsymbol{F}\boldsymbol{F}^T$, where $\boldsymbol{F}$ is the deformation tensor. A very special sub-class of the bodies defined by the above implicit relation are classical isotropic compressible Cauchy elastic bodies described with the following constitutive expression for the stress:

$$\boldsymbol{T} = \delta_0 \boldsymbol{I} + \delta_1 \boldsymbol{B} + \delta_2 \boldsymbol{B}^2, \tag{1.2}$$

where the material moduli depend on the density and the principal invariants of $\boldsymbol{B}$. We note that the above equation presents an explicit expression for the Cauchy stress in terms of the Cauchy-Green tensor.

A different set of constitutive relations is given by

$$\boldsymbol{B} = \alpha_0 \boldsymbol{I} + \alpha_1 \boldsymbol{T} + \alpha_2 \boldsymbol{T}^2, \tag{1.3}$$

where the material moduli are functions of the density and the principal invariants of the stress. Moon and Truesdell [11] have obtained conditions under which the representation (1.2) is invertible. However, they were considering the invertibility of isotropic functions and were not interested in delineating models of the form (1.3) that do not belong to (1.2), or to put it differently whether there are models of the form (1.3) that are not Cauchy elastic. It is important to recognize that many models belonging to the class defined by (1.3) do not belong to the class defined by (1.2).

While the linearization of (1.2) under the assumption that the displacement gradient is small leads to the classical linearized elastic model, linearizing (1.3) under the same assumption leads to the approximation

$$\boldsymbol{\varepsilon} = \beta_0 \boldsymbol{I} + \beta_1 \boldsymbol{T} + \beta_2 \boldsymbol{T}^2, \tag{1.4}$$

and thus it is possible for the linearized strain to bear a nonlinear relationship to the stress. Rajagopal [12] and Devendiran *et al.* [13] used models belonging to the above class to describe the response of titanium alloys. In this paper, we shall also use a power-law model that belongs to the above class of constitutive relations to describe the response of titanium alloys. Our model has fewer material constants than the model used by Devendiran *et al.* [13] to corroborate experimental data on titanium alloys. While Rajagopal [12] used a model with fewer material moduli to describe the response of Gum Metal, he did not describe the response of other titanium alloys. Here, we model numerous titanium alloys within the framework of the same form of constitutive relation, the only difference being the values for the material moduli.

## 2. Experimental data and the new class of constitutive relations

The recent studies by Rajagopal [12] and Devendiran *et al.* [13] have employed a new class of constitutive relations to corroborate the experimental data for tensile loading of beta-phase titanium alloys, see Saito *et al.* [3], Sakaguch *et al.* [4], Hao *et al.* [5], and Hou *et al.* [6].

A tensile loading experiment is described by the set of pairs $(\sigma^i, \eta^i)$, $i = \{1 \ldots N\}$. Each pair contains the value of strain $\eta^i$ corresponding to the loading stress $\sigma^i$. There is no loss of generality in assuming that the tensile stress is applied along the direction of the first Cartesian coordinate. Therefore, the stress tensor takes the form

$$\boldsymbol{T} = (\boldsymbol{e}_1 \otimes \boldsymbol{e}_1)\sigma = \begin{pmatrix} \sigma & 0 & 0 \\ 0 & 0 & 0 \\ 0 & 0 & 0 \end{pmatrix}, \tag{2.1}$$

where $T_{11} = \sigma$ is its only nonzero component[2]. We shall also identify the normal

[2]Symbol $\boldsymbol{e}_1$ denotes the unit vector in the direction of the first Cartesian coordinate and symbol $\otimes$ denotes the tensor product.

strain components $(\varepsilon_{11}, \varepsilon_{22}, \varepsilon_{33})$ with $(\eta, \gamma, \gamma)$, i.e., we assume that $\varepsilon_{22} = \varepsilon_{33}$. Note that to our best knowledge there are no data regarding the transverse strain $\gamma$.

The reversible elastic response of cold swagged Gum Metal can be observed up to the strains of 2.5%, see [3] and Fig. 1. Since the elastic response of Gum Metal and many other titanium alloys is in the range $|\varepsilon| < 0.025$, such strains could be regarded as large by researchers as most metals do not exhibit the elastic response for the magnitude of such strains. On the other hand, from the modeling point of view we can use the small displacement gradient approximation and model the response using the small strain tensor since the displacement gradient norm is so small that its square can be neglected in comparison to itself, see [12].

Two models were proposed by Rajagopal in [12] to fit the experimental data for cold swagged Gum Metal. The first model is a power-law model in which the strain is given by

$$\boldsymbol{\varepsilon} = \lambda_1 \operatorname{tr} \boldsymbol{T} \boldsymbol{I} + \lambda_2 (1 + \alpha \operatorname{tr} \boldsymbol{T}^2)^n \boldsymbol{T}, \tag{2.2}$$

where $\lambda_1$, $\lambda_2$, $\alpha$ and $n$ are the material moduli. The second, exponential model is of the form

$$\boldsymbol{\varepsilon} = \lambda_1 \operatorname{tr} \boldsymbol{T} \boldsymbol{I} + \lambda_2 \exp(\beta \operatorname{tr} \boldsymbol{T}) \boldsymbol{T}, \tag{2.3}$$

where $\lambda_1$, $\lambda_2$ and $\beta$ are the material moduli. For the uniaxial loading of the form (2.1), when setting $\lambda_1 = 0$, the model (2.3) reduces to

$$\begin{aligned} \eta &= \lambda_2 \sigma \exp(\beta \sigma), \\ \gamma &= 0. \end{aligned} \tag{2.4}$$

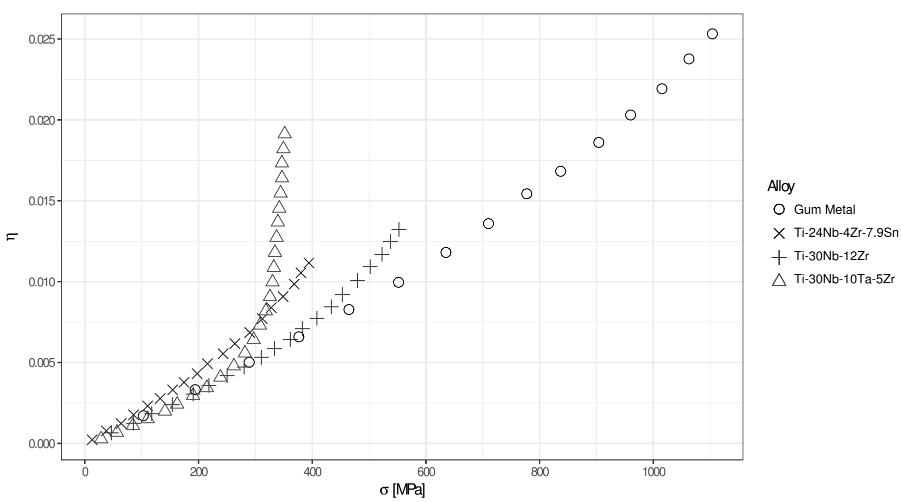


Fig. 1. Stress strain response to tensile loading of considered titanium alloys in the elastic regimen.

The actual material parameters that were used in [12] are

$$\lambda_2 = 1.57 \times 10^{-11}\ \mathrm{Pa}^{-1}, \qquad \beta = 3.22 \times 10^{-10}\ \mathrm{Pa}^{-1}. \tag{2.5}$$

The model (2.4) with the parameters (2.5) provides a very good agreement with experimental data, see Fig. 2. If we linearize this model around $\sigma = 0$, we obtain an estimate for Young's modulus

$$\frac{1}{E} = \frac{d\eta}{d\sigma}(0) = \lambda_2, \tag{2.6}$$

which yields

$$E = 63.7\ \mathrm{GPa}. \tag{2.7}$$

Devediran *et al.* [13] use two models to capture the response of beta-phase titanium alloys. One is a fully implicit model (that is not further discussed here) and the other is an explicit model for the linearized strain, namely

$$\boldsymbol{\varepsilon} = \beta_1 \operatorname{tr} \boldsymbol{T}\boldsymbol{I} + (\beta_2 + \beta_3 \exp{(1 + \beta_4 \operatorname{tr}{(\boldsymbol{T}^2)})^{\frac{n}{2}}})\boldsymbol{T}, \tag{2.8}$$

with the material moduli $\beta_1$, $\beta_2$, $\beta_3$, $\beta_4$ and $n$. For the uniaxial stress setting (2.1), under the assumption $\gamma := \varepsilon_{22} = \varepsilon_{33}$, the model (2.8) reduces to

$$\begin{aligned} \eta &= (\beta_1 + \beta_2 + \beta_3 \exp{(1 + \beta_4(\sigma^2))^{\frac{n}{2}}})\sigma, \\ \gamma &= \beta_1 \sigma. \end{aligned} \tag{2.9}$$

Here

$$E_\beta = \frac{1}{\beta_1 + \beta_2 + \beta_3 e}. \tag{2.10}$$

is the expression for Young's modulus for model (2.8). In [13], the model (2.9) was used to fit the experimental data of *Ti-30Nb-10Ta-5Zr* alloy, *Ti-24Nb-4Zr-7.9Sn* alloy and *Ti-30Nb-12Zr* alloy. For the values of material moduli of these alloys, we refer to [13, Table 2]. In Figs. 3, 4 and 5 the explicit model (2.9) is included as dashed line.

## 3. Fitting tensile loading experiments to power-law models

In this section, we corroborate the experimental data that is available for titanium alloys to a power-law model defined as

$$\boldsymbol{\varepsilon} = \frac{1}{9\hat{K}(|\operatorname{tr}(\boldsymbol{T})|^2)}(\operatorname{tr} \boldsymbol{T})\boldsymbol{I} + \frac{1}{2\hat{\mu}(|\boldsymbol{T}^d|^2)}\boldsymbol{T}^d, \tag{3.1}$$

where $\boldsymbol{T}^d = \boldsymbol{T} - \frac{1}{3}(\operatorname{tr}\boldsymbol{T})\boldsymbol{I}$ is the deviatoric part of stress, and the generalized bulk and shear moduli $\hat{K} = \hat{K}(|\operatorname{tr}(\boldsymbol{T})|^2)$ and $\hat{\mu} = \hat{\mu}(|\boldsymbol{T}^d|^2)$ are of the form

$$\begin{aligned} \hat{K}(|\operatorname{tr}(\boldsymbol{T})|^2) &= K\left(\frac{\tau_0^2}{\tau_0^2 + |\operatorname{tr}(\boldsymbol{T})|^2}\right)^{\frac{s-2}{2}} \\ \hat{\mu}(|\boldsymbol{T}^d|^2) &= \mu\left(\frac{\tau_0^2}{\tau_0^2 + \frac{3}{2}|\boldsymbol{T}^d|^2}\right)^{\frac{q-2}{2}}, \end{aligned} \tag{3.2}$$

where $\tau_0 > 0$, $q \in (1, \infty)$, $s \in (1, \infty)$, $\mu > 0$ and $K > 0$ are the material moduli. The parameter $s$ and the coefficient $K$ describe volume changes in response to the mean normal stress, while the parameter $q$ and the coefficient $\mu$ describe the isochoric part of deformation. We refer to parameters $K$ and $\mu$ as bulk and shear moduli, respectively. Note that we obtain Hooke's law with $\hat{K} = K$ and $\hat{\mu} = \mu$ upon setting $s = q = 2$ in (3.2). In addition, note that from (3.1) it follows that

$$\hat{K} = \frac{\operatorname{tr}(\boldsymbol{T})}{3\operatorname{tr}(\boldsymbol{\varepsilon})} \qquad \text{and} \qquad \hat{\mu} = \frac{|\boldsymbol{T}^d|}{2|\boldsymbol{\varepsilon}^d|}.$$

There is a reason for the decomposition of the stress as expressed in (3.1). Criscione and co-workers, see [14, 15], have shown that it is best to describe the experimental data for the stored energy using an integrity basis that is not collinear. That is, it is best to describe the stored energy using an integrity basis that captures the effect of shear and dilatation separately. The decomposition (3.1) is in keeping with such idea in that the stress response is split into a part that represents the volume change and the shear response.

Note that the parameter $\tau_0$ is chosen in such a manner that we are guaranteed that the response of the nonlinear model is reasonably close to the linearized model if $|\boldsymbol{T}|$ is small. This means that upon linearizing the model (3.1) around $\boldsymbol{T} = \boldsymbol{0}$, we obtain the classical linearized elastic model as long as

$$|\boldsymbol{T}| \ll \tau_0. \tag{3.3}$$

Finally, we also wish to remark that the model (3.1) can be put in the appropriate thermodynamic setting (see [9, 10, 16]). In particular, there is a (Gibbs) potential $\mathcal{G}(\boldsymbol{T})$ of the form (see also [17])

$$\mathcal{G}(\boldsymbol{T}) = \frac{1}{2}\int_0^{|\operatorname{tr}\boldsymbol{T}|^2} \frac{1}{9K}\left(\frac{\tau_0^2 + \xi}{\tau_0^2}\right)^{\frac{s-2}{2}} \mathrm{d}\xi + \frac{1}{2}\int_0^{|\boldsymbol{T}^d|^2} \frac{1}{2\mu}\left(\frac{\tau_0^2 + \frac{3}{2}\xi}{\tau_0^2}\right)^{\frac{q-2}{2}} \mathrm{d}\xi,$$

so that (3.1) can be written in the form

$$\boldsymbol{\varepsilon} = \frac{\partial \mathcal{G}}{\partial \boldsymbol{T}}.$$

Since $\mathcal{G}$ is strictly convex, there is a function $W$ depending on $\boldsymbol{\varepsilon}$ so that $\boldsymbol{T} = \frac{\partial W}{\partial \boldsymbol{\varepsilon}}$, its explicit form is however not known in general.

### 3.1. Procedure of corroborating experimental data

Since we assume that the Cauchy stress tensor $\boldsymbol{T}$ is of the form (2.1) and $T_{11} = \sigma$ is its only nonzero component, it immediately follows that

$$\boldsymbol{T}^d = \begin{pmatrix} \frac{2}{3}\sigma & 0 & 0 \\ 0 & -\frac{1}{3}\sigma & 0 \\ 0 & 0 & -\frac{1}{3}\sigma \end{pmatrix}, \qquad |\boldsymbol{T}^d| = \sqrt{\frac{2}{3}}\sigma, \qquad \operatorname{tr}\boldsymbol{T} = \sigma. \tag{3.4}$$

When fitting the tensile loading data to the model (3.1) with parameters $(\tau_0, s, q, K, \mu)$, the model reduces to

$$\begin{aligned} \eta &= \frac{1}{9K}\left(\frac{1}{\tau_0}\right)^{s-2}(\tau_0^2+\sigma^2)^{\frac{s-2}{2}}\sigma + \frac{1}{3\mu}\left(\frac{1}{\tau_0}\right)^{q-2}(\tau_0^2+\sigma^2)^{\frac{q-2}{2}}\sigma, \\ \gamma &= \frac{1}{9K}\left(\frac{1}{\tau_0}\right)^{s-2}(\tau_0^2+\sigma^2)^{\frac{s-2}{2}}\sigma - \frac{1}{6\mu}\left(\frac{1}{\tau_0}\right)^{q-2}(\tau_0^2+\sigma^2)^{\frac{q-2}{2}}\sigma. \end{aligned} \tag{3.5}$$

We use two approaches for fixing $\tau_0$ in (3.5). For all experimental data that we use $|\boldsymbol{T}|$ takes the values in the range of $10^7 - 10^9$ (10 MPa–1 GPa), and for $|\boldsymbol{T}| > 5.10^8$ the response is nonlinear, see Fig. 1. In the first approach, we set $\tau_0 = 5.10^8$ for all the materials that were studied. In the second approach, we set $\tau_0 = \sigma_{max}$, where $\sigma_{max}$ represents the maximal loading in the elastic regime; the explicit values for each titanium alloy are specified below in the first column of Table 2. In both approaches we always meet the assumption (3.3) in the linear regime.

Thus, upon fixing $\tau_0$, our model (3.5) is completely characterized by four parameters. The model (2.4) used by Rajagopal [12] to corroborate the experimental data for cold swagged Gum Metal has two parameters but as mentioned earlier the model was not used to corroborate the experiments on other titanium alloys other than Gum Metal, while the explicit model used by Devendiran *et al.* [13] to describe the tensile response of titanium alloys has five parameters.

For corroborating the experimental data that is available we use linear regression. We understand that Eq. $(3.5)_1$ for particular values of $(\tau_0, s, q)$ is a linear model of the form

$$\eta = c_1 f_1(\sigma) + c_2 f_2(\sigma), \tag{3.6}$$

where

$$f_1(\sigma) = \left(\frac{\tau_0^2+\sigma^2}{\tau_0^2}\right)^{\frac{s-2}{2}}\sigma, \qquad f_2(\sigma) = \left(\frac{\tau_0^2+\sigma^2}{\tau_0^2}\right)^{\frac{q-2}{2}}\frac{2}{3}\sigma. \tag{3.7}$$

Let $\sigma^i$, $i \in 1 \dots N$, represent the particular experimental tensile stress and $\eta^i$, $i \in 1 \dots N$ represent the observations of the strain. The values of functions $f_1(\sigma^i)$ and $f_2(\sigma^i)$ are understood as independent variables and the value of the strain $\eta^i$ is understood as the observed value. Using linear regression we obtain estimates for the coefficients $c_1$ and $c_2$ in (3.6) and derive estimates of the bulk and shear moduli

$$K = \frac{1}{9c_1}, \qquad \mu = \frac{1}{2c_2}. \tag{3.8}$$

Using this procedure we can estimate optimal values of the parameters $K$ and $\mu$ for a given $(\tau_0, s, q)$. Since the parameter $\tau_0$ is fixed, we need to estimate optimal values of the exponents $s$ and $q$. We decided to perform this estimation by comparing the quality of fit for different pairs $(s, q)$. For measuring the quality of fit in the model we need the following definitions:

DEFINITION 1 (Mean of observations).

$$\overline{\eta} = \frac{1}{N} \sum_{i=1}^{N} \eta^i. \tag{3.9}$$

DEFINITION 2 (Total sum of squares).[3]

$$S_{tot} = \sum_{i=1}^{N} (\eta^i - \overline{\eta})^2. \tag{3.10}$$

DEFINITION 3 (Residual sum of squares).

$$S_{res} = \sum_{i=1}^{N} (\eta^i - (c_1 f_1(\sigma^i) + c_2 f_2(\sigma^i)))^2. \tag{3.11}$$

DEFINITION 4 (Coefficient of determination $R^2$).

$$R^2 = 1 - \frac{S_{res}}{S_{tot}}. \tag{3.12}$$

The coefficient of determination $R^2 \leq 1$ is a standard measure of the quality of fit in the linear regression. The closer the value of the coefficient of determination is to 1, the better the fit is.

[3]For linear models without intercept, as is the case (3.6), the formula (3.10) for the total sum of squares is often used with $\overline{\eta} = 0$. We decided to use the formula (3.10) involving $\overline{\eta}$ in order to obtain more realistic coefficients of determination $R^2$.

**3.2. Implementation**

We outline the algorithm used for fitting a tensile loading data for an alloy to the model (3.6) as follows:

- We fix some particular value of $\tau_0$, derived from a characteristic magnitude of stress for which the response can be modeled as linear for small strain tending to zero.
- We choose an admissible set of the model parameters $(s, q)$. In particular, we use $s \in \{1.01, 1.02, \ldots, 100\}$, $q \in \{1.01, 1.02, \ldots, 100\}$. The values of $s$ and $q$ are discrete values from the finite sequence $\{1.01, 1.02, \ldots, 100\}$ of numbers incremented by 0.01.
- For each admissible pair of $(s, q)$ we obtain estimates of the coefficients $(c_1, c_2)$ of the model (3.6) using linear regression of the experimental data. From (3.12) we get the value of the coefficient of determination $R^2$.
- We choose the pair $(s, q)$ that maximizes the coefficient of determination $R^2$ among all admissible pairs of the model exponents.
- For the pair $(s, q)$ that maximizes $R^2$, we substitute the least square estimate of $(c_1, c_2)$ into Eq. (3.8) to compute the parameters $K$ and $\mu$ of the model. By this procedure we obtain **the best fit** $(\tau_0, s, q, K, \mu)$.

Without any additional assumption, the best fit is not unique as the alternative choice to the best fit $(\tau_0, s, q, K, \mu)$ of the form $(\tau_0, q, s, \frac{\mu}{3}, 3K)$ fits the tensile test data identically. To fix this apparent ambiguity, we have added an extra condition to the algorithm, namely

$$|s - 2| > |q - 2|. \tag{3.13}$$

If we assume that, instead of (3.13), the condition is

$$|s - 2| \leq |q - 2|, \tag{3.14}$$

then the corresponding linearized elastic model will have a negative Poisson's ratio, which contradicts the experiments. This issue is illustrated below, see Table 3 and Fig. 12. A more detailed analysis can be found in [18].

## 4. Results

The best fit obtained by the algorithm outlined above maximizes the coefficient of determination and minimizes the residual sum of squares among all admissible pairs of $(s, q)$. Linear regression was performed using the function `lm` from the R software environment and language, see [19, 20]. Source code of the algorithm has been deposited to https://bitbucket.org/kulvait/fittingtitanium-alloys.

In Tables 1 and 2, we present the values of the best fit for each titanium alloy studied, assuming the validity of the condition (3.13). Table 1 lists the material moduli when $\tau_0 = 5.10^8$. Table 2 lists the material moduli when $\tau_0 = \sigma_{max}$ specified in the first column of Table 2. In Table 4, we compare the quality of the obtained fits with the fits for the models (2.4) and (2.9) considered in [12, 13]. In Table 3, we present the values of the best fit when assuming (3.14) instead of (3.13), and as the outcome we observe that Poisson's ratio is negative, which contradicts the experiments. Thus the condition (3.13) eliminates physically irrelevant values.

**Table 1. The values of the best fit, Young's modulus $E$ and Poisson's ratio $\nu$ for $\tau_0 = 0.5GPa$; these values are achieved under the assumption $|s-2| > |q-2|$.**

| Alloy | $\tau_0$ | $s$ | $q$ | $K$ | $\mu$ | $R^2$ | $E$ | $\nu$ |
|---|---|---|---|---|---|---|---|---|
| Gum Metal | 0.5 GPa | 7.65 | 2.23 | 6223 GPa | 20.2 GPa | 0.9998 | 60.5 GPa | 0.50 |
| *Ti-30Nb-10Ta-5Zr* | 0.5 GPa | 9.15 | 2.49 | 334 GPa | 22.3 GPa | 0.9998 | 65.6 GPa | 0.47 |
| *Ti-24Nb-4Zr-7.9Sn* | 0.5 GPa | 15.68 | 2.99 | 1126 GPa | 16.5 GPa | 0.9997 | 49.3 GPa | 0.49 |
| *Ti-30Nb-12Zr* | 0.5 GPa | 56.49 | 4.29 | 180252 GPa | 25.1 GPa | 0.9980 | 75.4 GPa | 0.50 |

**Table 2. The values of the best fit, Young's modulus $E$ and Poisson's ratio $\nu$ for $\tau_0$ specified in the first column; these values are achieved under the assumption $|s-2| > |q-2|$.**

| Alloy | $\tau_0$ | $s$ | $q$ | $K$ | $\mu$ | $R^2$ | $E$ | $\nu$ |
|---|---|---|---|---|---|---|---|---|
| Gum Metal | 1.1 GPa | 28.5 | 2.82 | 1283552 GPa | 20.0 GPa | 0.9999 | 60.1 GPa | 0.50 |
| *Ti-30Nb-10Ta-5Zr* | 0.6 GPa | 9.81 | 2.58 | 291 GPa | 22.4 GPa | 0.9998 | 65.5 GPa | 0.46 |
| *Ti-24Nb-4Zr-7.9Sn* | 0.4 GPa | 12.13 | 2.65 | 1201 GPa | 16.5 GPa | 0.9997 | 49.4 GPa | 0.49 |
| *Ti-30Nb-12Zr* | 0.4 GPa | 37.89 | 3.39 | 804644 GPa | 25.7 GPa | 0.9980 | 77.0 GPa | 0.50 |

**Table 3. The values of the best fit, Young's modulus $E$ and Poisson's ratio $\nu$ for $\tau_0$ specified in the first column; these values are obtained under the assumption $|s-2| \le |q-2|$.**

| Alloy | $\tau_0$ | $s$ | $q$ | $K$ | $\mu$ | $R^2$ | $E$ | $\nu$ |
|---|---|---|---|---|---|---|---|---|
| Gum Metal | 0.5 GPa | 2.23 | 7.65 | 6.7 GPa | 18668 GPa | 0.9998 | 60.5 GPa | -1.00 |
| *Ti-30Nb-10Ta-5Zr* | 0.5 GPa | 2.49 | 9.15 | 7.4 GPa | 1001 GPa | 0.9998 | 65.6 GPa | -0.97 |
| *Ti-24Nb-4Zr-7.9Sn* | 0.5 GPa | 2.99 | 15.68 | 5.5 GPa | 3378 GPa | 0.9997 | 49.3 GPa | -0.99 |
| *Ti-30Nb-12Zr* | 0.5 GPa | 4.29 | 56.49 | 8.4 GPa | 540755 GPa | 0.9980 | 75.4 GPa | -1.00 |

In Figs. 2–5 there is a comparison of the best fit of the power law model (3.5) for $\tau_0 = 5.10^8$ with the predictions of the explicit models considered in [12] and [13] when fitting the axial strain $\eta$.

**Table 4. Comparison of the quality of fit characterized by the coefficient of determination $R^2$ and Young's modulus estimates $E$ between the power-law model (3.5) (see the third and second to the last columns in Tables 1–3) and the models (2.4) and (2.9) studied earlier in [12, 13]. Here, $R^2$ is the coefficient of determination for the models (2.4) and (2.9), $E$ is the estimate of Young's modulus for the model (2.4) for Gum Metal and for the model (2.9) for the remaining titanium alloys.**

| Material | $R^2$ | $E$ |
|---|---|---|
| Gum Metal | 0.9982 | 63.7 GPa |
| *Ti-30Nb-10Ta-5Zr* | 0.9997 | 63.8 GPa |
| *Ti-24Nb-4Zr-7.9Sn* | 0.9996 | 48.1 GPa |
| *Ti-30Nb-12Zr* | 0.9966 | 75.6 GPa |

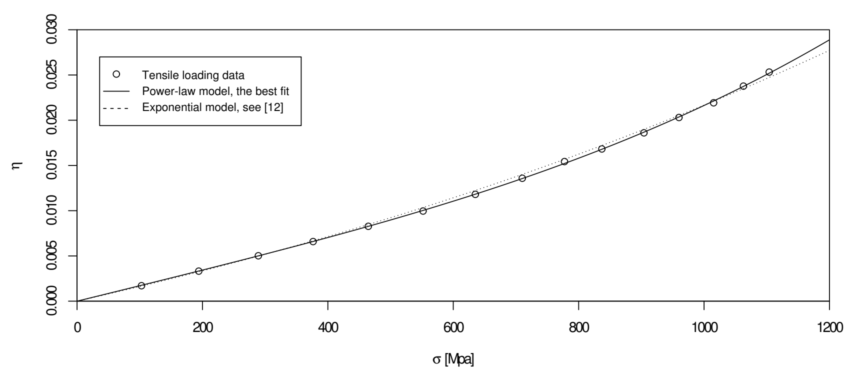


FIG. 2. Plot of the best fit for the model (3.5) compared with the exponential model (2.4) for Gum Metal, see [12].

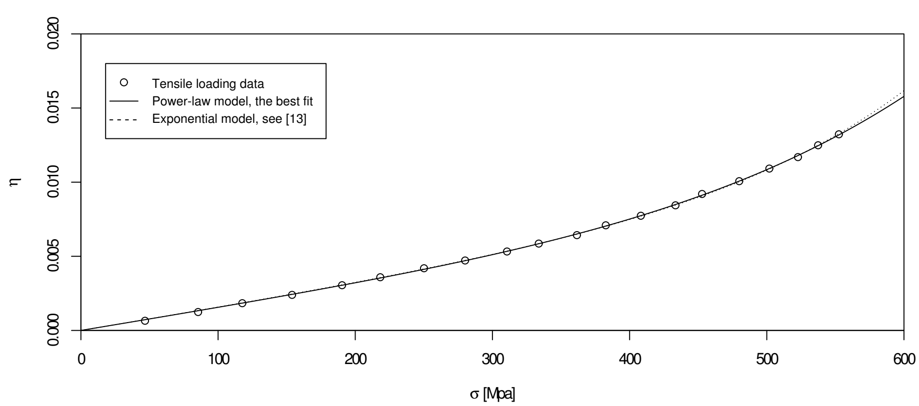


FIG. 3. Plot of the best fit for the model (3.5) compared with the exponential model (2.9) for *Ti-30Nb-10Ta-5Zr*, see [13].

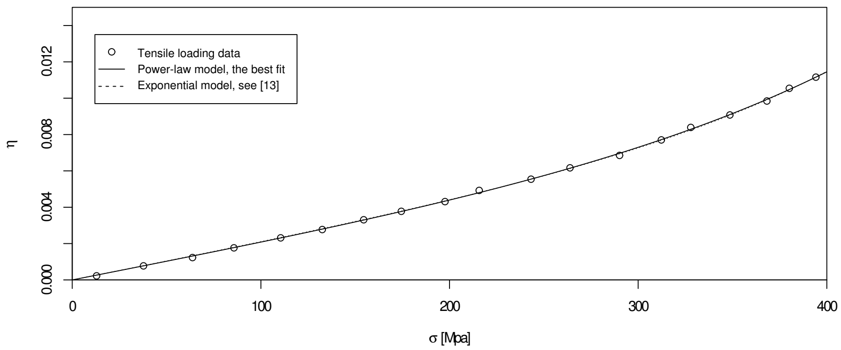


Fig. 4. Plot of the best fit for the model (3.5) compared with the explicit exponential model (2.9) for *Ti-24Nb-4Zr-7.9Sn*, see [13].

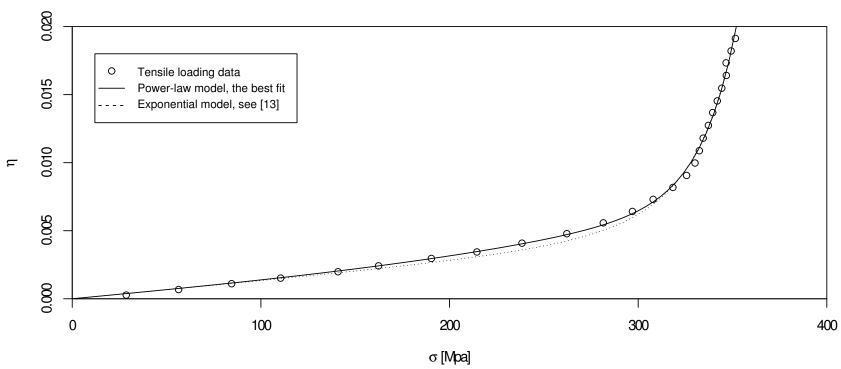


Fig. 5. Plot of the best fit for the model (3.5) compared with the explicit exponential model (2.9) for *Ti-30Nb-12Zr*, see [13].

**4.1. Predicted bulk and shear responses of power-law model**

A set of values $(\tau_0, s, q, K, \mu)$ associated with the best fit can be used to predict character of the response for general deformation based on the equations (3.1) and (3.2). The bulk and shear responses take the form

$$\operatorname{tr}\boldsymbol{\varepsilon} = \frac{1}{3K}\left(\frac{\tau_0^2 + |\operatorname{tr}\boldsymbol{T}|^2}{\tau_0^2}\right)^{\frac{s-2}{2}} \operatorname{tr}\boldsymbol{T}, \tag{4.1a}$$

$$|\boldsymbol{\varepsilon}^d| = \frac{1}{2\mu}\left(\frac{\tau_0^2 + \frac{3}{2}|\boldsymbol{T}^d|^2}{\tau_0^2}\right)^{\frac{q-2}{2}} |\boldsymbol{T}^d|. \tag{4.1b}$$

In Figs. 6–9 we plot these predicted bulk and shear responses for Gum Metal, *Ti-30Nb-10Ta-5Zr*, *Ti-24Nb-4Zr-7.9Sn*, and *Ti-30Nb-12Zr* respectively with the best fit data listed in Table 1. In Fig. 10 we compare the bulk responses (4.1a) in tension and in compression for all studied alloys.

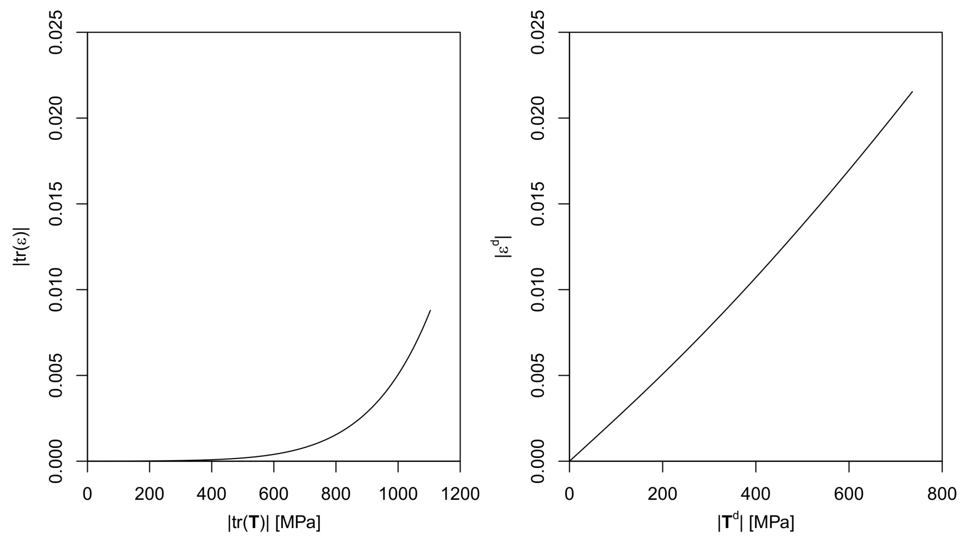


Fig. 6. Bulk and shear response (4.1) of the model (3.1)–(3.2) for Gum Metal.

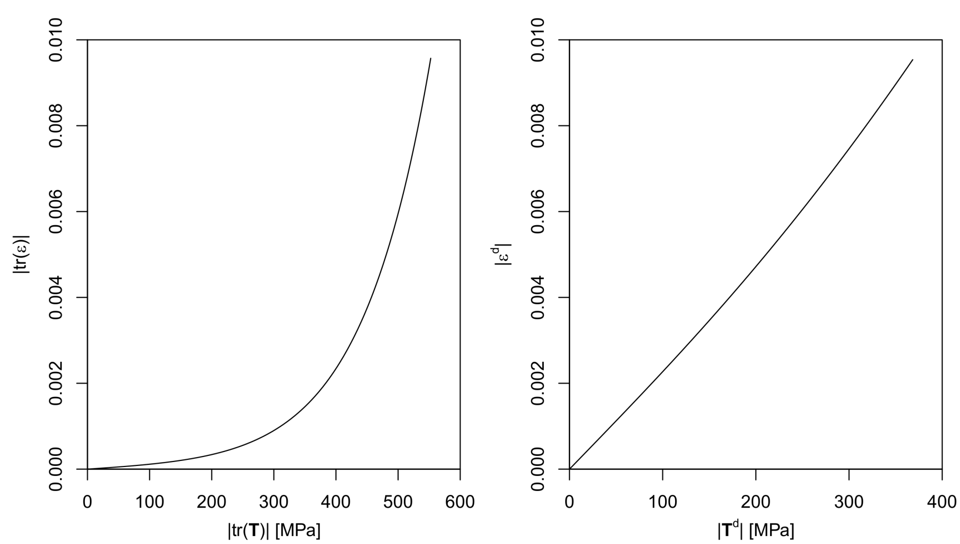


Fig. 7. Bulk and shear response (4.1) of the model (3.1)–(3.2) for *Ti-30Nb-10Ta-5Zr* alloy.

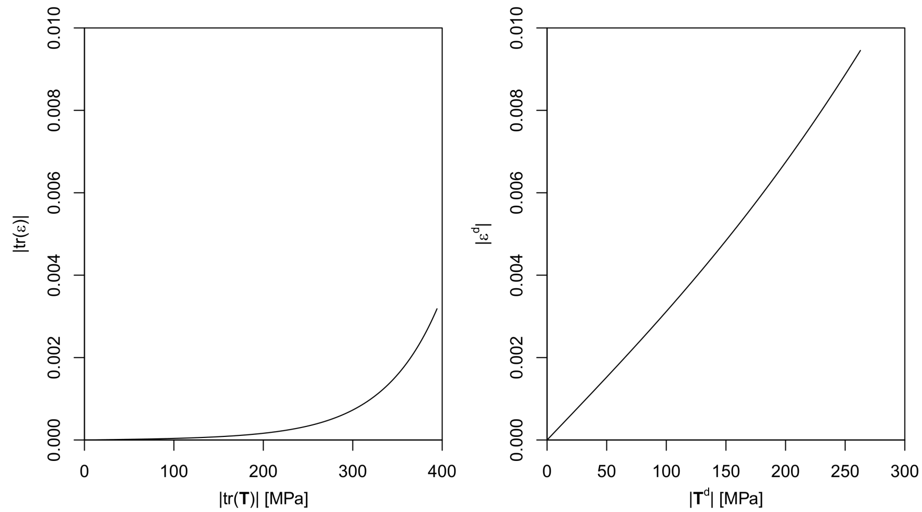


FIG. 8. Bulk and shear response (4.1) of the model (3.1)–(3.2) for *Ti-24Nb-4Zr-7.9Sn* alloy.

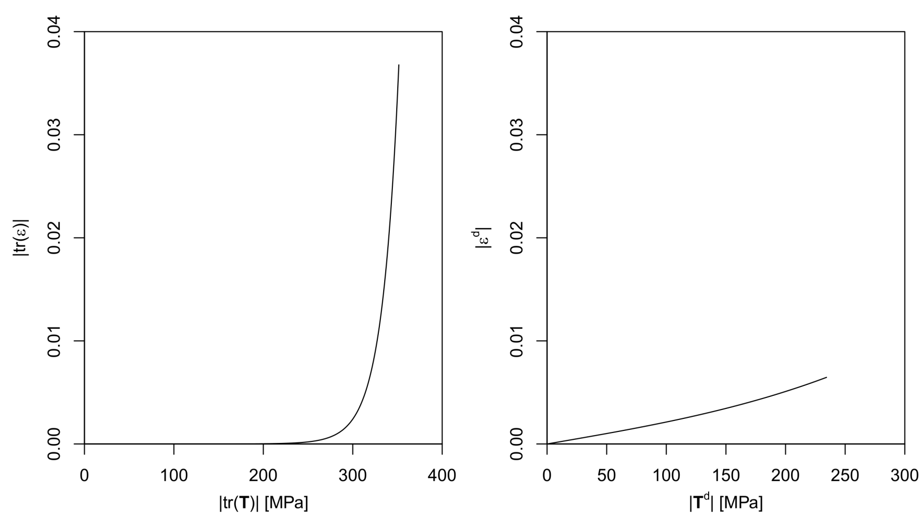


FIG. 9. Bulk and shear response (4.1) of the model (3.1)–(3.2) for *Ti-30Nb-12Zr* alloy.

In a simple tension, we are also interested in the behavior of the ratio

$$\hat{\nu}(\sigma) = -\gamma(\sigma)/\eta(\sigma).$$

It can be expressed from (3.5) as follows:

$$\hat{\nu}(\sigma) = -\frac{\gamma(\sigma)}{\eta(\sigma)} = -\frac{\frac{1}{9K}\left(\frac{1}{\tau_0}\right)^{s-2}\left(\tau_0^2+\sigma^2\right)^{\frac{s-2}{2}} - \frac{1}{6\mu}\left(\frac{1}{\tau_0}\right)^{q-2}\left(\tau_0^2+\sigma^2\right)^{\frac{q-2}{2}}}{\frac{1}{9K}\left(\frac{1}{\tau_0}\right)^{s-2}\left(\tau_0^2+\sigma^2\right)^{\frac{s-2}{2}} + \frac{1}{3\mu}\left(\frac{1}{\tau_0}\right)^{q-2}\left(\tau_0^2+\sigma^2\right)^{\frac{q-2}{2}}}. \tag{4.2}$$

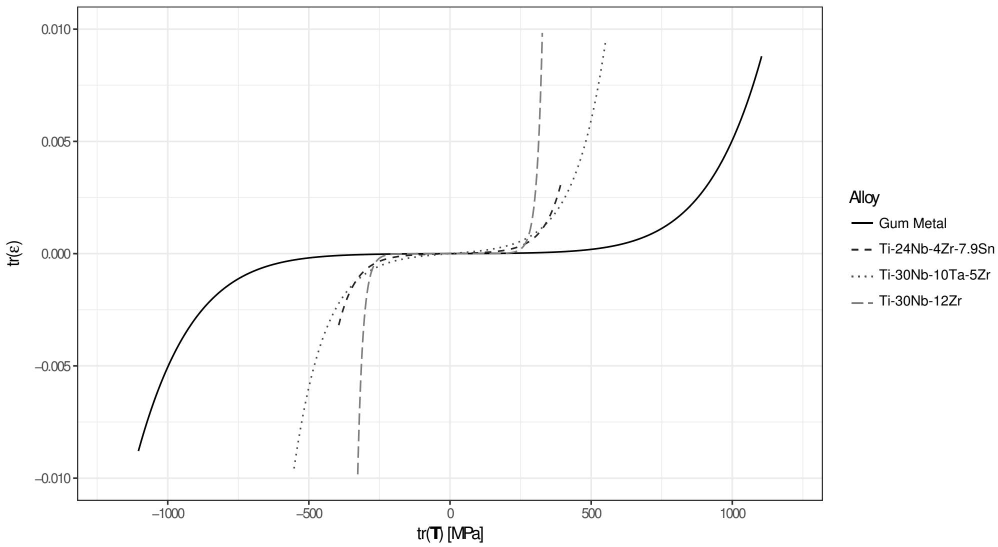


Fig. 10. Bulk responses (4.1a) for all alloys under the assumption $|s-2| > |q-2|$.

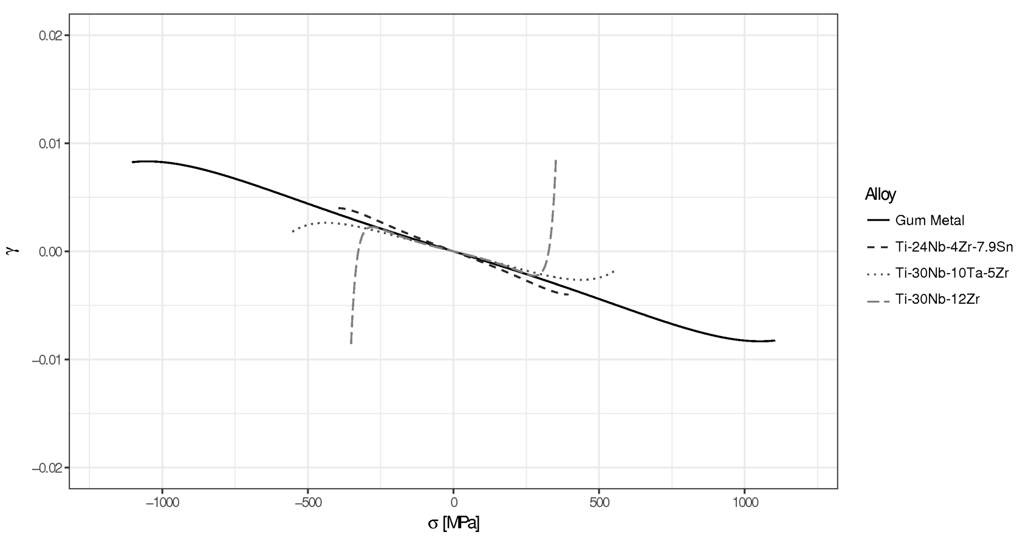


Fig. 11. Transversal strain $\gamma$ for all alloys under the assumption $|s-2| > |q-2|$.

Letting $\sigma \to 0$ in Eq. (4.2), we obtain Poisson's ratio

$$\nu = \frac{3K - 2\mu}{2(3K + \mu)}. \tag{4.3}$$

The plot of the dependence of $\gamma$ on $\sigma$ is given in Fig. 11 for all studied alloys.

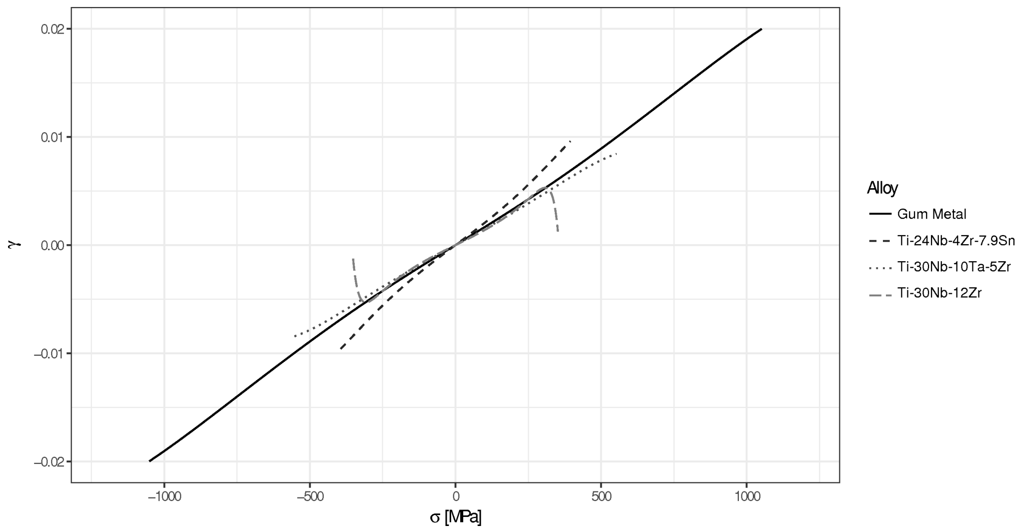


FIG. 12. Transversal strain $\gamma$ under the assumption $|s-2| < |q-2|$.

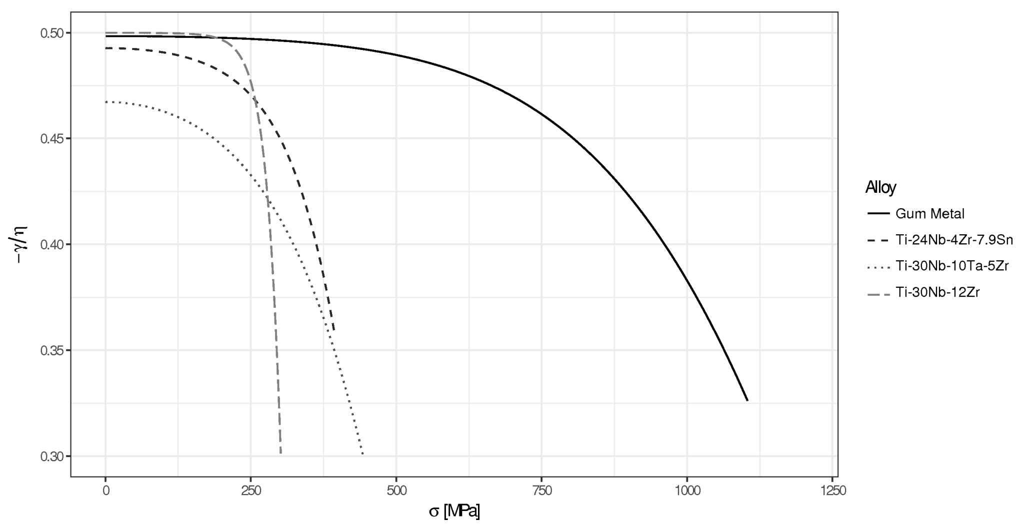


FIG. 13. The ratio $-\gamma/\eta$ (4.2) for all alloys under the assumption $|s-2| > |q-2|$.

We recall that these results are for the best fit values fulfilling (3.13). For the sake of completeness, we also add, in Fig. 12, the plot of the dependence of $\gamma$ on $\sigma$ for the best fit values satisfying the alternative condition (3.14). Figure 12 confirms that the setting fulfilling (3.14) is incorrect, because it predicts positive transversal strains $\gamma$. In Fig. 13 we show the graph of function $\hat{\nu}$ defined in (4.2) for all the alloys under the condition (3.13).

### 4.2. Discussion and concluding remarks

All beta titanium alloys that have been studied behave nonlinearly in their small strain regime. Thus it would be inappropriate to describe them using the linearized elastic model, see Figs. 2–5.

We have considered a class of power-law models where the nonlinear dependence of the strain on the deviatoric part of the stress and its trace are mutually separated and can have different polynomial growth. As pointed out by Criscione and his co-workers, see [14, 15], such decomposition is more appropriate for capturing experimental data as the experiments focus on measuring the effect of shear, dilatation, etc., separately.

We have observed that the power-law models are able to describe the tensile loading behavior of Gum Metal and other beta-phase titanium alloys in the full range of nonlinear elastic response as can be seen from Figs. 2–5. It is also evident from Tables 1 and 4 that the power-law model (3.1) outperforms or at least is as good as the existing models considered in [12] and [13] for describing the tensile loading behavior of the beta-phase titanium alloys. There is a compelling reason for our choice of the exponents. If we reverse the exponents and assume that $|s-2| < |q-2|$, then the transversal strain $\gamma$ is (in tensile loading) positive and Poisson's ratio is negative, which contradicts the available data, see Table 3 and Fig. 12. The parameter $\tau_0$ has been set up a priori in such a way that the models are close to the classical linearized model if $|\boldsymbol{T}|$ is much smaller than $\tau_0$.

In the performed corroboration of the experimental data, the coefficient of determination $R^2$ is very close to the ideal value of 1 for all the above mentioned models, see Table 1. Of course, one needs to consider more general deformations in order to validate the model, but such experiments are not available with regard to the metallic alloys being considered at this point in time.

## Acknowledgements

This work has been supported by the ERC-CZ project LL1202 financed by the Ministry of Education, Youth and Sports of the Czech Republic.

## References

1. N. Nagasako, R. Asahi, J. Hafner, *First-principles Study of Gum-Metal Alloys: Mechanism of Ideal Strength*, R&D Review of Toyota CRDL, **44**, 61–68, 2013.

2. R.J. Talling, R.J. Dashwood, M. Jackson, D. Dye, *On the mechanism of superelasticity in Gum metal*, Acta Materialia, **57**, 1188–1198, 2009.

3. T. Saito, T. Furuta, J.H. Hwang, S. Kuramoto, K. Nishino, N. Suzuki, R. Chen, A. Yamada, K. Ito, Y. Seno, T. Nonaka, H. Ikehata, N. Nagasako, C. Iwamoto, Y. Ikuhara, T. Sakuma, *Multifunctional alloys obtained via a dislocation-free plastic deformation mechanism*, Science, **300**, 464–467, 2003.

4. N. Sakaguch, M. Niinomi, T. Akahori, *Tensile deformation behavior of Ti-Nb-Ta-Zr biomedical alloys*, Materials Transactions, **45**, 1113–1119, 2004.

5. Y.L. Hao, S.J. Li, S.Y. Sun, C.Y. Zheng, Q.M. Hu, R. Yang, *Super-elastic titanium alloy with unstable plastic deformation*, Applied Physics Letters, **87**, 91906–91906, 2005.

6. F.Q. Hou, S.J. Li, Y.L. Hao, R. Yang, *Nonlinear elastic deformation behaviour of Ti-30Nb-12Zr alloys*, Scripta Materialia, **63**, 54–57, 2010.

7. K.R. Rajagopal, *On implicit constitutive theories*, Applications of Mathematics, **48**, 279–319, 2003.

8. K.R. Rajagopal, *The elasticity of elasticity*, Zeitschrift für angewandte Mathematik und Physik, **58**, 309–317, 2007.

9. K.R. Rajagopal, A.R. Srinivasa, *On the response of non-dissipative solids*, Proceedings of the Royal Society A: Mathematical, Physical and Engineering Sciences, **463**, 357–367, 2007.

10. K.R. Rajagopal, A.R. Srinivasa, *On a class of non-dissipative materials that are not hyperelastic*, Proceedings of the Royal Society A: Mathematical, Physical and Engineering Sciences, **465**, 493–500, 2009.

11. H. Moon, C. Truesdell, *Interpretation of adscititious inequalities through the effects pure shear stress produces upon an isotropic elastic solid*, Archive for Rational Mechanics and Analysis, **55**, 1–17, 1974.

12. K.R. Rajagopal, *On the nonlinear elastic response of bodies in the small strain range*, Acta Mechanica, **225**, 1545–1553, 2014.

13. V.K. Devendiran, R.K. Sandeep, K. Kannan, K.R. Rajagopal, *A thermodynamically consistent constitutive equation for describing the response exhibited by several alloys and the study of a meaningful physical problem*, International Journal of Solids and Structures, **108**, 1–10, 2017.

14. J.C. Criscione, J.D. Humphrey, A.S. Douglas, W.C. Hunter, *An invariant basis for natural strain which yields orthogonal stress response terms in isotropic hyperelasticity*, Journal of the Mechanics and Physics of Solids, **48**, 2445–2465, 2000.

15. J.C. Criscione, *Rivlin's representation formula is ill-conceived for the determination of response functions via biaxial testing*, [in:] The Rational Spirit in Modern Continuum Mechanics, C.-S. Man, R.L. Fosdick [Eds.], Springer Netherlands, pp. 197–215, 2004.

16. C. Bridges, K.R. Rajagopal, *Implicit constitutive models with a thermodynamic basis: a study of stress concentration*, Zeitschrift für angewandte Mathematik und Physik, **66**, 191–208, 2014.

17. M. Bulíček, J. Málek, K.R. Rajagopal, E. Süli, *On elastic solids with limiting small strain: modelling and analysis*, EMS Surv. Math. Sci, **1**, 293–342, 2014.

18. V. Kulvait, *Mathematical analysis and computer simulations of deformation of nonlinear elastic bodies in the small strain range*, Charles University, Faculty of Mathematics and Physics, Prague, Ph.D. Thesis, 2017.

19. R Development Core Team, *R: A Language and Environment for Statistical Computing, Reference Index*, http://cran.r-project.org/doc/manuals/r-release/fullrefman.pdf, 2016 (available online).

20. J.M. Chambers, T. Hastie, *Statistical Models in S*, Wadsworth & Brooks/Cole Advanced Books & Software, 1992.

*Received March 15, 2017; revised version May 31, 2017.*